J Therm Anal Calorim (2012) 107:763–776
DOI 10.1007/s10973-011-1515-8

Thermal and mass spectral characterization of novel azo dyes of p-acetoamidophenol in comparison with Hammett substituent effects and molecular orbital calculations

M. A. Zayed · Gehad G. Mohamed · M. A. Fahmey

Received: 25 January 2011 / Accepted: 17 March 2011 / Published online: 11 April 2011

Abstract Four novel azo compounds were synthesized: o-phenylazo-($C_{14}H_{13}N_3O_2$) (I), p-bromo-o-phenylazo-($C_{14}H_{13}BrN_3O_2$) (II), p-methoxy-o-phenylazo-($C_{15}H_{16}N_3O_3$) (III), and p-nitro-o-phenylazo-p-acetamidophenol ($C_{14}H_{13}N_4O_4$) (IV). These compounds were carefully investigated using elemental analyses, IR, and thermal analyses (TA) in comparison with electron ionization (EI) mass spectral (MS) fragmentation at 70 eV. Semi-empirical MO calculation, PM3 procedure, has been carried out on the four azo dyes (I–IV), both as neutral molecules and the corresponding positively charged molecular ions. These included molecular geometries (bond length, bond order, and charge distribution, heats of formation, and ionization energies). The mass spectral fragmentation pathways and thermal decomposition mechanisms were reported and interpreted on the basis of molecular orbital (MO) calculations. They are found to be highly correlated to each other. Also, the Hammett's effects of p-methoxy, p-bromo, and p-nitro-substituents of phenyl azo groups on the thermal stability of these dyes (I–IV) are studied by experimental (TA and MS) in comparison with MO calculations, and the data obtained are discussed. This research aimed chiefly to throw more light on the structures of the four prepared azo derivatives of acetoamidophenol (p-cetamol). The data refering to the thermal stability of these dyes can be used in industry for effective dyeing purposes under different thermal conditions.

M. A. Zayed (✉) · G. G. Mohamed
Chemistry Department, Faculty of Science, Cairo University, Giza 12613, Egypt
e-mail: mazayed429@yahoo.com

M. A. Fahmey
Nuclear Physics Department, N.R.C., Atomic Energy Authority, Cairo 13759, Egypt

Keywords Acetamidophenol azodyes · Hammett effect · FT-IR · Mass spectrometry · Thermal analyses · MO-calculations

Introduction

Azo dyes are the most versatile class of dyes [1], and thermal analysis plays an important role in studying their structures [2]. The applicability of the dyes for special uses and determining thermal stabilities of them are also very important [2]. The resistance to heat at elevated temperatures is one of the main properties required from dyes used in high temperature processes such as dyeing, printing, and photo-copying and in high technology areas such as lasers, electro-optical devices etc. [3]. Most of the previous studies on the physical and chemical properties studies of mono-azo dyes were carried out in solution. Very few studies in the literature have reported showing the relationship between thermal stabilities and structures of azo dyes [4]. The research available in the literature reporting on azo dyes containing sterically hindered groups such as tert-butyl, sec-butyl, and isopropyl is also scarce [5]. Only the thermal behavior of some azo dyes containing sterically hindered and water-soluble group have been previously reported [6].

Mass spectrometry plays pivotal role in the structural characterization of organic molecules [7]. The technique is important because it provides a lot of structural information of the sample with a low cost. Also, this technique offers comparative advantages in terms of speed and productivity for organic analysis [8]. On the other hand, thermal analysis technique delivers extremely sensitive measurements of heat change which can be applied on a broad scale with

organic development. These methods provide unique information related to thermodynamic data of the system studied [9]. The increasing use of these techniques combined with TA will be able to provide more specific information, and thus facilitate more rapid interpretation of the obtained curves [9].

In electron ionization (EI) mass spectrometry, the fragmentation consists of competitive and consecutive unimolecular fragmentation [10]. The fragmentation of ionized molecule depends mainly on its internal energy [11]. The thermo-gravimetric TG/DTG analysis was used for providing quantitative information on weight losses due to decomposition and/or evaporation of low molecular materials as a function of time and temperature. In conjunction with mass spectrometric analysis [12–19], the nature of the released volatilized material may be deduced, thus greatly facilitating the interpretation of thermal stability and/or degradation processes. On the other hand, computational quantum chemistry provides additional information about the atoms and bonds, which can be used successfully in an interpretation of experimental results [20]. This helps in the description and prediction of primary fragmentation site of cleavage and subsequent one [16–19].

The aim of this study is to carry out experimental and theoretical investigation of the four azo compounds of the biologically active p-cetamol drug using thermal analyses (TA) measurements and EI mass spectral (MS) fragmentation at 70 eV. Also, molecular orbital (MO) calculations are performed using PM3 procedure, on the neutral molecule and charged molecular ion to investigate bond length, bond order, heats of formation, ionization energy, and charge distribution. These calculations are correlated with the experimental results (TA and MS) to obtain indication about the stability of the studied compounds and prediction of the site of primary fragmentation step and subsequent ones. Also, the results of the analyses are used to discuss the effect of Hammet values of substituents on experimental and computational results.

Experimental

Preparation of the p-acetoamidophenol-azodyes (I–IV) and characterization

The p-acetoamidophenol-derivatives (I–IV) were prepared by coupling p-acetoamidophenol with phenyl, bromo-, methoxy-, and nitro diazonium chloride, in an ice bath, in the presence of sodium hydroxide [20]. The precipitates were left in refrigerator overnight, filtered and crystallized from acetic acid (yield 86–89%). Their elemental analyses (for C, H, and N) were performed in Microanalytical Center, Cairo University. Their structures were investigated by elemental analyses, IR, electron ionization mass spectra (EI-MS), and Thermal analyses (TGA, DTG, and DTA).

Elemental analyses, FT-IR, EI-MS, and thermal analyses

Elemental microanalyses of the separated solid dyes for C, H, N, and S were performed in the Microanalytical Center, Cairo University, using CHNS-932 (LECO) Vario Elemental Analyzers. Infrared spectra were recorded on a Perkin-Elmer FT-IR type 1650 spectrophotometer in the wave number region of 4000–400 cm^{-1}. The spectra were recorded as KBr pellets.

The EI-MS of the studied dyes (I–IV) were obtained using Shimadzu GC-MS-Qp 1000 PX quadruple mass spectrometer with electron multiplier detector equipped with GC-MS data system. EI-MS were obtained at ionizing energy value of 70 eV, ionization current of 60 μA, and in vacuum better than 10^{-6} torr.

The thermal analyses of the studied dyes (I–IV) were made using conventional thermal analyzer (Shimadzu system of DTA-50 and 30 series TGA-50). The mass losses of 5 mg sample and heat reopens of the change of the sample were measured from room temperature up to 500 °C. The heating rate, in an inert argon atmosphere, was 10 °C min^{-1}. These instruments were calibrated using indium metal as a thermal stable material. The reproducibility of the instrument reading was determined by repeating each experiment more than twice.

Molecular orbital calculations

The MO-calculations were performed using the parametric method (PM3) described by Stewart [21]. The default criteria for terminating all optimizations were increased by a factor of 100 (keyword PRECISE). Vibrational frequencies were computed for the studied structures (keyword FORCE) so as to check whether the newly designed geometries are local minima. All the MO calculations were carried out at the restricted Hartree–Fock level (RHF) for the neutral molecular compounds (used in TA); while the unrestricted Hartree–Fock level (UHF) were carried out for there positively charged ions (utilized in MS) using PM-3 method followed by full optimization of all geometrical variables (bond lengths, bond angles, and dihedral angles), without any symmetry constraint. All structures were optimized to a gradient normalization of 0.01–0.05, using the eigenvector following (EF) routine [22]. All the semi-empirical MO calculations were performed with the MOPAC2000 software package [23] implemented on an Intel Pentium IV 3.0 GHz computer.

Results and discussion

Structure elucidation of prepared dyes by elemental analyses and FT-IR

The elemental analyses of the prepared dyes referred to the general formulae of o-phenylazo-($C_{14}H_{13}N_3O_2$) (I) (Found C = 57.98%, H = 4.35%, and N = 7.54%, and Calcd. C = 66.14%, H = 4.72%, and N = 16.53%), p-bromo-o-phenylazo-($C_{14}H_{13}BrN_3O_2$) (II) (Found C = 42.2%, H = 2.95%, Br = %, and N = 7.53%, and Calcd C = 50.31%, H = 3.89%, Br = 23.92%, and N = 12.57%), p-methoxy-o-phenylazo-($C_{15}H_{16}N_3O_3$) (III) (Found C = 60.30%, H = 5.29%, and N = 7.05%, and Calcd. C = 63.15%, H = 5.61%, and N = 14.73%) and p-nitro-o-phenylazo-p-acetoamidophenol ($C_{14}H_{13}N_4O_4$) (IV) (Found C = 54.34%, H = 3.89%, and N = 14.05%, and Calcd. C = 56.00%, H = 4.33%, and N = 18.66%) compounds, respectively. The given structural formulae of these dyes are confirmed by FT-IR (Table 1).

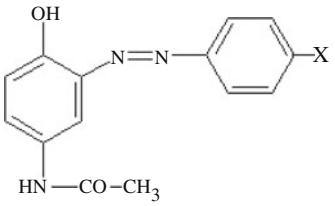

X = H, Br, O-CH_3, and NO_2

For dyes I-IV

Structural formulae of dyes I–IV

The data (Table 1) refer to assignment of main bands of the active groups in the moiety of these dyes, such as 510–618, 1173–1310, 1419–1595, 1657, 3028–3056, and 3284–3560 cm^{-1} for *v*C–N amide, C–O amide, *v*CH_3 amide, *v*N=N azo, *v*CO amide, *v*OH phenolic, and *v*NH amide in dye I, respectively. The positions of these bands are varied from one dye to another because of the variation of donating power effect of p-substituents of phenyl azo group. Extra bands appeared at 515–585 cm^{-1} for *v*C–Br

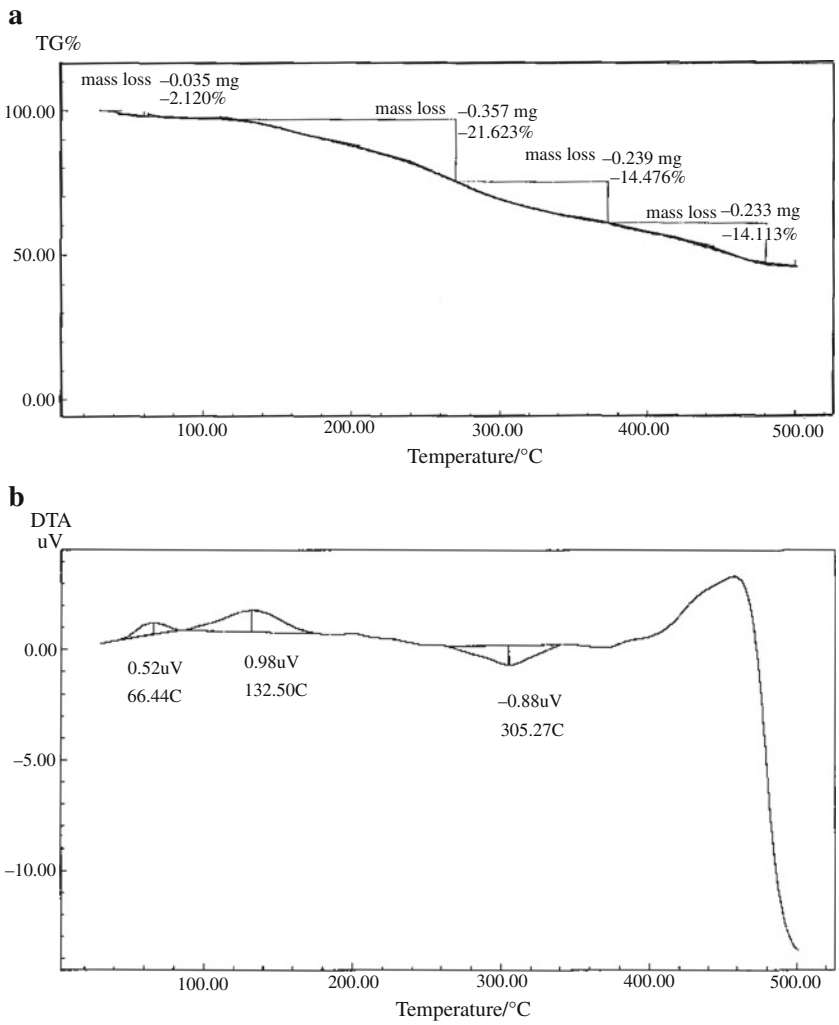

Fig. 1 **a** TG of dye I, (**b**) DTA of dye I

Table 1 The FT-IR spectral data description of p-acetoamidophenol azo derivatives/I–IV

Compound	Wave number/cm^{-1}	Description
I	510–618	δC–N amid, C–O amid
	1173–1310	νCH_3 amide
	1419–1595	νN=N azo
	1657	νCO amide
	3028–3056	νOH phenolic
	3284–3560	νNH amide
II	515–585	νC–Br, νC–O amid
	1007–1068	νCH_3 amide
	1420–1664	νN=N
	1663	νCO amide
	3087	νOH phenolic
	3284–3684	νNH amide
III	511–585	δC–N amide, νC–O
	1105–1203	νCH_3 amide
	1426–1666	νN=N
	1666	νCO amide
	3108	νOH phenolic
	3321–3648	νNH amide
IV	522–640	νC–O amid, νN–O
	1490–1560, 1310–1360	νNO_2, δNO_2
	1176–1293	νCH_3 amide
	1660	νCO amide
	1439–1660	νN=N
	2835–3069	νOH phenolic
	3291–3600	νNH amide

I: o-phenylazo-pacetoamidophenol, II: p-bromo-o-phenylazo-p-acetoamidophenol, III: p-methoxy-o-phenylazo-p-acetoamidophenol, IV: p-nitro-o-phenylazo-p-acetoamidophenol

in case of dye II, and at 1560–1490 and 1360–1310 cm^{-1} of νNO_2 in case of dye IV.

Knowledge of thermal decomposition mechanism of the dye is very important to understand the chemical processes. It is difficult to establish the exact major fragmentation pathway in EI using conventional MS. However, combination of the experimental techniques (TA and MS) and MO calculation is very important to understand the following topics:

1. Primary site fragmentation process and its major fragmentation pathway in both techniques.
2. Stability of the studied compounds as neutral molecules in solid-state phase and molecular ions in gas phase.
3. Selection of the most probable decomposition pathways in vitro system using both TA and MS.
4. Substituent effect of p-methoxy, p-bromo, and p-nitro o-phenylazo groups on experimental and computational results.

Thermal decomposition interpretation

The description of thermal decomposition of azo dyes (I–IV) under investigation is given in Table 2 and Figs. 1, 2, 3, 4. From the data obtained for dye I (Fig. 1), it is clear that o-phenylazo-p-actamidophenol (I) decomposed in two main steps, the first step (at 25–260 °C) is due to the loss of $NOCH_3$ group (Pract. % = 23.7, Calcd. = 23.35%), the second step (at 260–500 °C) is due to the loss of C_6H_5 radical (Pract. = 29.59% and Calcd. = 30.20%). The remaining part containing azo group is present up to temperature more than 500 °C. These losses appeared in DTG (Fig. 1a) at 275 and 377 °C. The DTA (Fig. 1c) data in respect of several exo- and endothermic peaks may be assigned to a series of physical and chemical changes (Scheme 1) occurring during thermal heating of the dye (I). The dye II TG, DTG, and DTA (Table 2; Fig. 2) show two steps (Fig. 2a): the first at temperature ranges 25–300 °C, and the second at 300–500 °C with practical mass losses of 27.17% (Calcd. = 28.0%) and Pract. = 18.02% (Calcd. = 17.91%), respectively. These mass losses are observed as two peaks in DTG (Fig. 2b) at 282.9 and 448.3 °C and in DTA (Fig. 2c) as endothermic peaks at 282.1 and 242.45 °C, respectively. The remainder part still keeps the azo group up to temperature >500 °C.

The dye III TG (Fig. 3a), DTG (Fig. 3b), and DTA (Fig. 3c) refer to the thermal decomposition of this dye in two steps. The first occurs at 25–310 °C due to the loss p-methoxyphenyl radical (Pract. Loss = 37.46% and Calcd. = 37.76%) and the second one occurs at 310–500 °C due to the loss of $CO + N_2$ gases (Pract loss = 20.95% and Calcd. = 20.0%). These losses appear at 274.16 and 475.55 °C in DTG (Fig. 3b) and at 265.54 and 455.95 °C in DTA (Fig. 3c) as endothermic peaks, respectively. The appearance of some endo- and exothermic peaks may be attributed to weight losses and chemical recombination to give the gases in the second step. This means that azo group of this compound decomposed at temperature range 300–500 °C.

The TG/DTA the dye IV (Fig. 4) were displayed within the temperature range 25–500 °C. It is clear from the thermal survey of this compound, that it has two main steps of mass losses in TGA (Fig. 4a). The first one appeared at the temperature range 25–360 °C with practical mass loss % = 35.08. This loss may be attributed to the decomposition of NO_2 as a gaseous molecule together with an acetic acid molecule (Calcd. = 35.21%). The second mass loss appeared at the temperature range 360–500 °C with mass loss % = 25.07. The second loss may be attributed to the decomposition of C_6H_5 radical (Calcd. Loss = 25.24%). These mass losses observed at two main peaks in DTG at 287.83 and 387.0 °C (Fig. 4b) and confirmed by the appearance of a series of exothermic and endothermic

Table 2 Thermal analyses description of acetoamidophenol-azodyes/I-IV

Compound and mole mass	TG temperature range/°C	DTG peak temperature/°C	Wt loss Found %/Calcd.%	Wt loss description	DTA temperature range/°C	DTA peak temperature/°C	DTA description
Dye I, 254	100–260	42.39	23.74/22.44	$-NCOCH_3$	40–70	66.44	Broad exo peak
	260–360	162.6			80–140	132.5	Broad exo peak
	360–480	275.1			260–320	305.2	Endo therm. peak
		377	28.59/29.92	$-C_6H_4$	380–460	440.4	Exo therm. peak
Dye II, 333.9	25–90	36.8	27.12/28.42	HBr + 1/2 N_2	25–70	40.16	Endo therm. peak
	90–290	282.9			70–120	93.55	Endo therm. Peak
	290–500	448.3	18.18/17.96	$-CH_3COOH$	140–180	183.18	Endo therm. Peak
					205–265	242.45	Endo therm. Peak
Dye III, 285	25–90	73.21	37.46/37.89	$-C_6H_5OCH_3$	25–140	75.74	Endo therm. peak
	90–320	274.16			280–330	309.65	Endo therm. Peak
	320–500	475.55	20.95/19.64	–CO + N_2	360–380	365.54	Sharp endo peak
					420–480	455.95	Endo therm. peak
Dye IV, 300	25–350	95.29	35.08/35.33	$-NO_2 + CH_3COOH$	60–100	99.93	Sharp endo peak
	350–500	287.83			160–200	194.42	Sharp endo peak
		387.07			240–300	270.18	Sharp exo peak
		475.50	25.07/24.66	$-C_6H_4$	320–380	351.04	Sharp endo peak
					380–500	439.90	Broad endo peak

I: o-phenylazo-p-acetoamidophenol, II: p-bromo-o-phenylazo-p-acetoamidophenol, III: p-methoxy-o-phenylazo-p-acetamidophenol, IV: p-nitro-o-phenylazo-p-acetoamidophenol

peaks in DTA (Fig. 4c). The remainder part still keeps azo group up to temperature >500 °C.

Therefore, it is generally concluded that thermal stability of these azodyes as a function of starting decomposition temperature and remaining of azo group till high temperature range; may be ordered as: dye III < dye I < dye II < dye IV depending on the Hammett's substituents values of −0.27, 0.01, 0.23 and 0.78, respectively (Table 3).

Mass spectral fragmentation and Hammett's substituents effects

The EI-MS of the four dyes (I–IV) at 70 eV are represented in Figs. 5, 6, 7, 8. The signal appeared in the mass spectra of dyes I, II, III, and IV at m/z = 255, 333, 286, and 300 are due to the formation of molecular ions, ($C_{14}H_{13}N_3O_2^+$, RI = 25%), ($C_{14}H_{13}N_3O_2Br^+$, RI = 23.8%), ($C_{15}H_{16}N_3O_3^+$, RI = 20%), and ($C_{14}H_{13}N_4O_4^+$, RI = 15.3%) for these dyes, respectively. The appearance of these molecular ions confirms their proposed general formula and agrees well with their elemental analyses. In case of dye I (Fig. 5) mass spectra refer to the appearance of mole fragments in three pathways. The signals appeared at m/z = 58 (RI = 50%) due to fragment ion $COOCH_2$, 77 (RI = 100%, base peak) due to fragment ion $C_6H_5^+$, the fragment ions containing azo group appeared at m/z = 105 (RI = 60%) due to C_6H_6–N_2^+, and at 165 (RI = 60%) due to CH_3CO–C_6H_4 (OH)–N = NH. The appearance of the fragment ions containing azo group of high RI of 60% refer to the stability of azo dye I even at high energy ionization source of 70 eV. In case of dye II (Fig. 6), its mass spectrum shows fragmentation of this dye in three parallel pathways. It shows in path I, fragment ions at m/z = 253 (RI = 1%) after the loss of HBr from the molecular ion; at m/z = 211 (RI = 16%) due fragment ion containing azo group; at m/z = 291 (RI = 29.8%) in path containing also azo group; and at m/z = 150 (RI = 100% base peak) containing no azo group. The low RI values of fragment ions containing azo group may refer to the low stability of p-bromoazodye II on its ionization with the high energy electron beam of 70 eV. In case of p-methoxy azo dye III its mass fragmentation occurs in three pathways which are given by Fig. 7. It shows three fragment ions containing azo group of m/z = 245 (RI = 30%) and m/z = 105 (RI = 23%), and m/z = 226 (25%). The middle values of RI % of these fragment ions containing azo group may refer to the middle stability of p-methoxyazo dye III. It is finally decomposed to give the fragment ion of m/z = 151 (RI = 60%) of p-acetoamidophenol parent compound and m/z = 77 (RI = 100%) as a base peak of $C_6H_5^+$ stable fragment ion. The EI-MS of p-nitroazodye IV are represented in Fig. 8. It

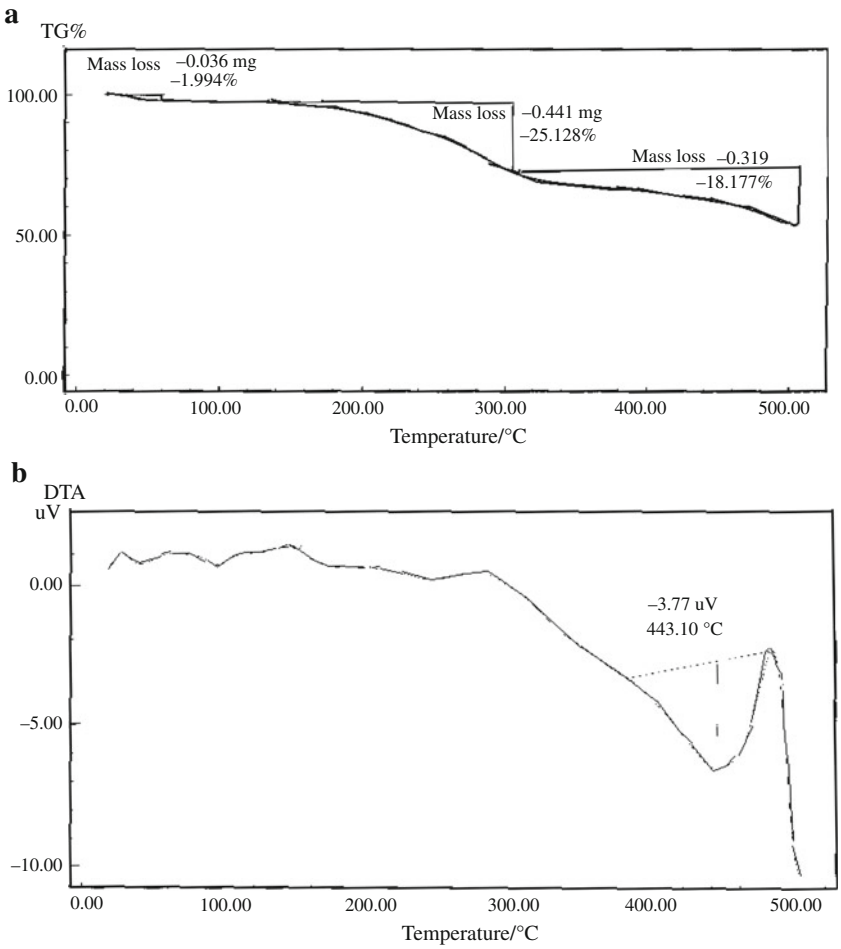

Fig. 2 **a** TG of dye II, (**b**) DTA of dye II

shows three fragment ions containing azo groups. These are at $m/z = 254$ (RI = 1%), at $m/z = 212$ (RI = 28%), and at $m/z = 258$ (RI = 12.5%). The last one fragment ion is the only one containing p-nitro-azogroup. The lower RI% values may refer to the instability of p-nitro-azodye IV in a similar way like p-bromoazodye II. This means that the electron withdrawing substituents are weakening the azo-dye stability. Therefore, the stability of these dye during ionization with 70 eV electron beam may be ordered as dye I > dye III > dye II > dye IV. This agrees well with the Hammett's values in relation to some MOCs parameters such as heat of formation, dipole-moment, electron affinity, and ionization potential (Table 3).

MO calculations and Hammett's substitution effects

The MO calculations give valuable information about the structure and the reactivity of a molecule and its molecular ions. Computational data can be used to support the experimental data. The much import parameters calculated using MO calculation are geometries, bond order, bond strain, charge distribution, heat of formation and ionization energy.

Investigation of the molecular structure of dyes I–IV is of interest in this study aiming to help in the illumination of experimental data (i.e., prediction of the weakest bond cleavage and the stability of the neutral molecule as well as molecular ion).

Figure 9 shows the numbering system of four dyes skeleton that helps in ordering the calculated bond order and charge distribution (different atoms) of both neutral and charged species. The calculated geometrical parameters are shown in Tables 3, 4, 5, 6, 7. The values of computed ionization energies, heats of formation dipole moment values in comparison with Hammet's constant values are given in Table 4.

The molecular orbital calculation parameters of dye I in neutral form related to thermal analysis are given in Tables 3 and 4. The data obtained in Table 3 refer to the dipole moment = 2.435 (Debye), heat of formation = 4.683 (KJ mol^{-1}), electron affinity = 0.43 (eV), ionization potential = 8.53 (eV), and Hammet's constant of 0.01. The data obtained in Table 4 refer to the order of increasing stability of bonds as C16–C17 < C3–N9 < C5–N11 < N11–C16 < N13–C19 < N9–N13. This means that the first cleavage bond is C16–C17 followed by C3–N9,

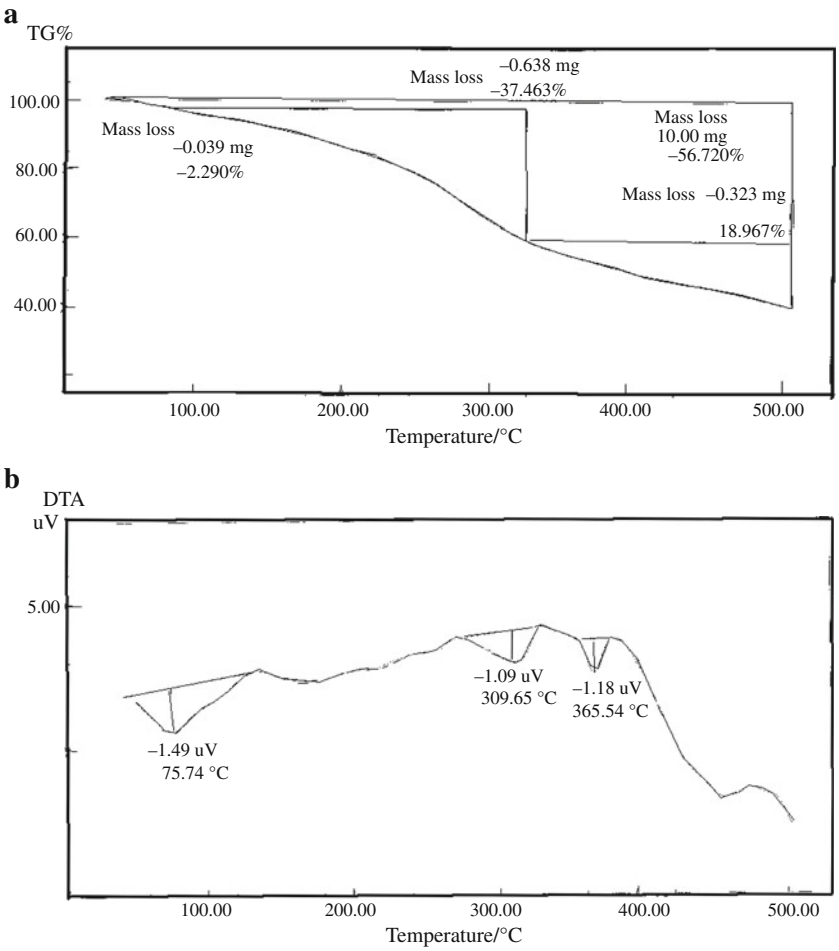

Fig. 3 **a** TG of dye III, (**b**) DTA of dye II

N13–C19, and N11–C16. The most stable bonds are azo group (N9–N13) and C16–O18.

The MO calculation parameters of dye I in ionic form related to mass spectra are given in Table 3. These data show that, the heat of formation of dye I in cationic form = 184.371 (KJ mol^{-1}), dipole moment = 6.160 (Debye), electron affinity = 4.421 (eV), and ionization potential = 12.71 (eV). These values differ greatly from those of the neutral form.

The MO calculation parameters of dye II in neutral form related to thermal analysis are given in Tables 3. The data obtained refer to the dipole moment = 2.257 (Debye), heat of formation = 12.519 (KJ mol^{-1}), electron affinity = 0.672 (eV), ionization potential = 8.61 (eV), and Hammet's constant of 0.23. The MOCs data obtained in Tables 3 and 5 of dye II, refer to the order of increasing stability of bonds in this dye as C16–C17 < C22–Br25 < C3–N9 < C5–N11 < N13–C19 < N11–C16 < N9–N13. This means that the first cleavage bond is C16–C17, C22–Br25 followed by C3–N9, C5–N11, N13–C19, and N11–C16. The most stable bonds are azo group (N9–N13) and the highly stable bond is C16–O18. The MO calculation parameters of dye II in ionic form related to mass spectra are given in Table 3. These data show that, the heat of formation of dye II in cationic form = 193.633 (KJ mol^{-1}), dipole moment = 15.942 (Debye), electron affinity = 4.482 (eV), and ionization potential = 12.78 (eV). These values differ greatly from those of the neutral form which is essentially related to the substituents effect of p-Br group in both forms.

The MO calculation parameters of dye III in neutral form related to thermal analysis are given in Table 3. The data obtained refer to the dipole moment = 1.335 (Debye), heat of formation = −33.659 (KJ mol^{-1}), electron affinity = 0.721 (eV), ionization potential = 8.51 (eV), and Hammet's constant of −0.27. The MOCs data obtained in Tables 3 and 6 of dye III, refer to the order of increasing stability of bonds in this dye as C16–C17 < N11–C16 < O25–C26 < C3–N9 < N13–C19 < C5–N11 < N9–N13. This means that the first cleavage bond is C16–C17 followed by N11–C16, O25–C26, C3–N9, and N13–C19. The most stable bonds are azo group (N9–N13) and its neighbor bond C5–N11. Also, there is another stable bond C16–O18. The MO calculation parameters of dye III in ionic form related to mass spectra are given in Table 3. These data show that, the heat of

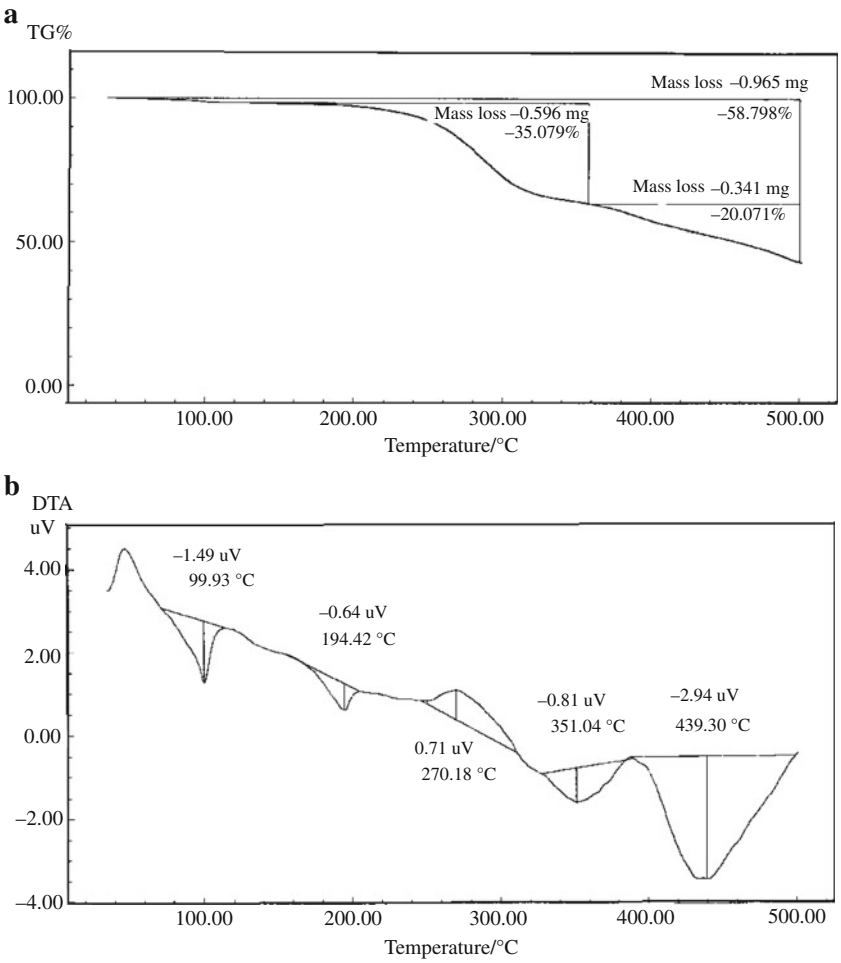

Fig. 4 **a** TG of dye IV, (**b**) DTA of dye IV

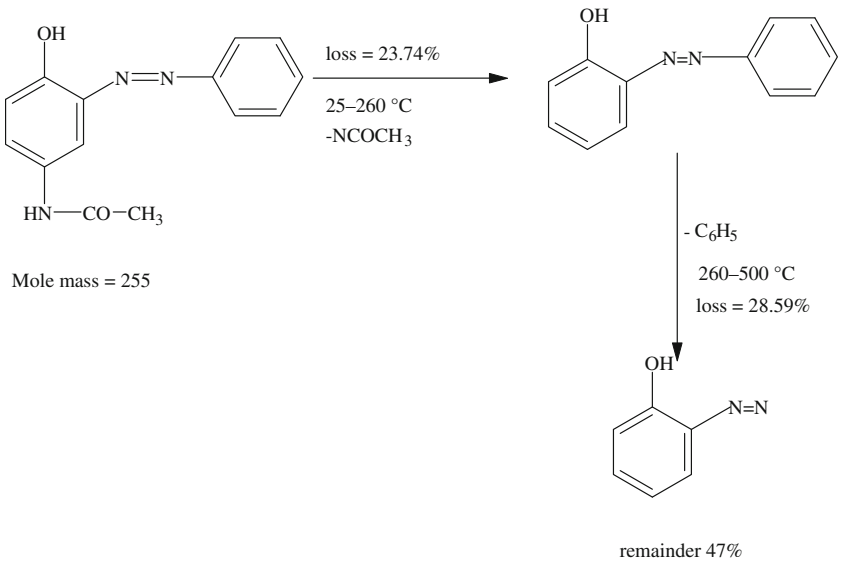

Scheme 1 Thermal decomposition scheme of dye I

formation of dye III in cationic form = 144.964 (KJ mol^{-1}), dipole moment = 8.707 (Debye), electron affinity = 4.333 (eV), and ionization potential = 12.62 (eV). These values differ greatly from those of the neutral form which is essentially related to the substituents effect of p-OCH_3 group in both forms.

The MO calculation parameters of dye IV in neutral form related to thermal analysis are given in Table 3. The

Table 3 Thermal decomposition DTG temperatures of dyes I–IV neutral molecules in comparison with molecular orbital calculations parameters

The dye no. and state	Heat of formation[b]/ kJ mol^{-1}	Dipole moment/ Debye[b]	Electron affinity/eV[b]	Ionization potential/eV[b]	DTG temperature of mass loss/°C	Hammett's[a] constant values
I, p–H						
a-Neutral state	4.683	2.435	0.433	8.53	275.12, 377.0	0.01
b- cationic state	184.371	6.160	4.421	12.71		
II, p-Br						
a-Neutral state	12.519	2.257	0.672	8.61	282.93, 483.03	0.23
b-Cationic state	193.633	15.942	4.482	12.78		
III, p-OCH_3						
a- Neutral state	−33.659	1.335	0.721	8.51	274.16, 475.55	−0.27
b-Cationic state	144.964	8.707	4.333	12.62		
IV, p-NO_2						
a-Neutral state	−4.497	6.094	1.608	9.04	277.83, 490.0	0.78
b-Cationic state	181.990	17.920	4.705	13.03		

[a] Reference [20]

[b] Molecular Orbital Calculation data using PM3 program

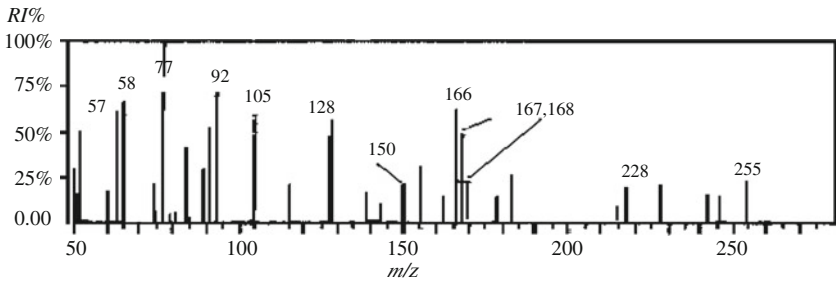

Fig. 5 EI-MS of dye I

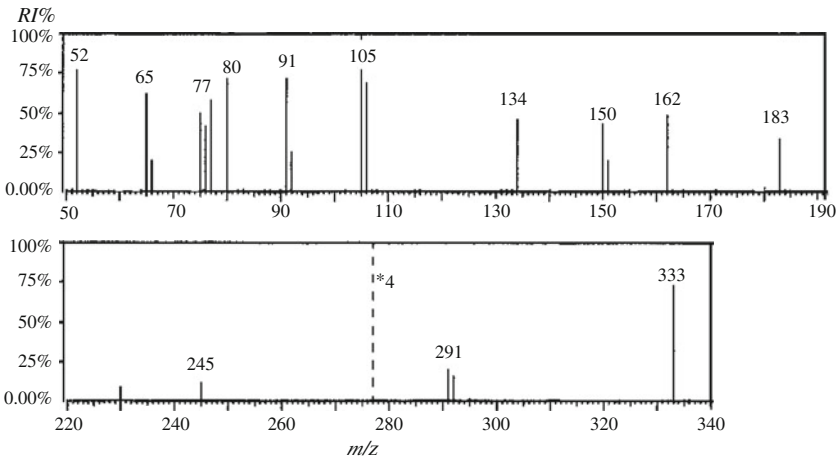

Fig. 6 EI-MS of dye II

data obtained refer to the dipole moment = 6.094 (Debye), heat of formation = −4.497 (KJ mol^{-1}), electron affinity = 1.608 (eV), ionization potential = 9.04 (eV), and Hammet's constant of 0.78. The MOCs data obtained in Tables 3 and 7 of dye IV, refer to the order of increasing stability of bonds in this dye as C22–N25 < N11–

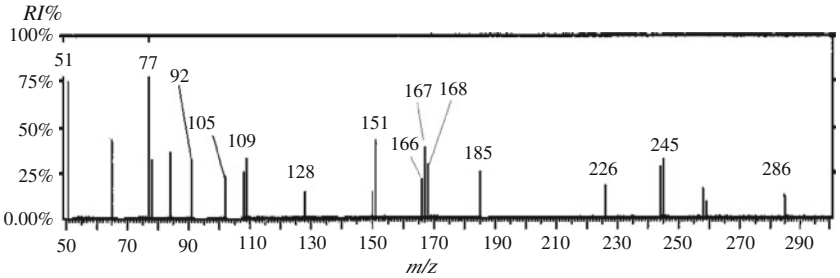

Fig. 7 EI-MS of dye III

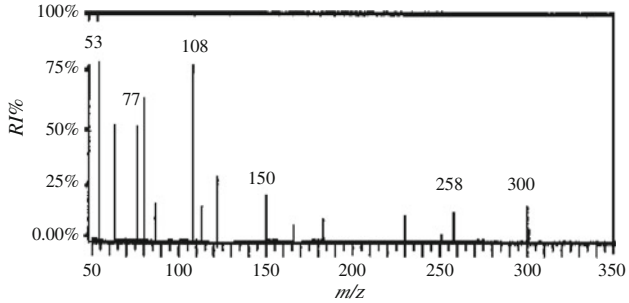

Fig. 8 EI-MS of dye IV

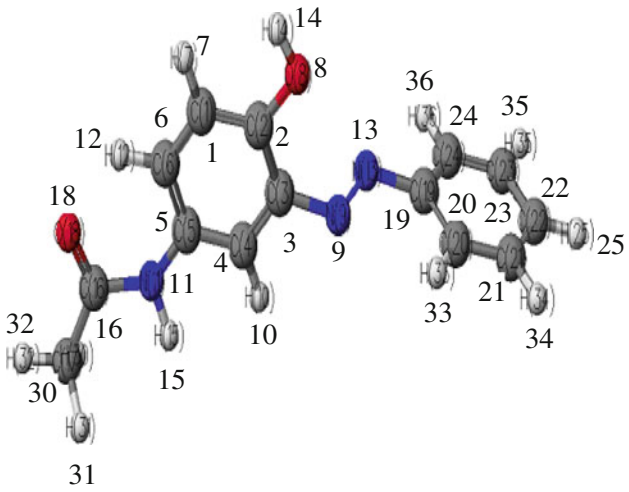

Fig. 9 Numbering system of dyes I–IV

C16 < C16–C17 < C3–N9 < N13–C19 < N9–N13. This means that the first cleavage bond is C22–N25 followed by N11–C16, C16–C17, C3–N9, and N13–C19. The most stable bonds are azo group (N9–N13) and its neighbor bond C5–N11. Also there are other stable bonds C16–O18, N25–O38, and N25–O37 of nitro group. The MO calculation parameters of dye IV in ionic form related to mass spectra are given in Table 3. These data show that, the heat of formation of dye IV in cationic form = 181.990 (KJ mol^{-1}), dipole moment = 17.920 (Debye), electron affinity = 4.705 (eV), and ionization potential = 13.03 (eV). These values differ greatly from those of the neutral form which is essentially related to the substituents effect of p-NO_2 group in both forms.

Comparison between TA and MO-calculations

The scope of this investigation is restricted to a search or prediction and discerns features of initial bond ruptures during the course of fragmentation of dyes (I–IV) molecules. Empirical observations indicate that the course of subsequent fragmentation is determined to large extent by the initial bond ruptures of the molecular ion in MS [24]. It is quite reasonable to say that the computational quantum chemistry can provide additional data which can be used successfully to interpret both TA and MS experimental results. These theoretical data will, particularly, be valuable for mass spectrometry scientists; in which the

Table 4 The molecular orbital calculation parameters of neutral form of dye I

Dye I neutral	Atom	Atom ID	Partial charge	Bond	Bond length/Å	Bond order
	O8	8	−0.222	C2–O8	1.369	1.059
	N9	9	0.002	C3–N9	1.453	0.988
	N11	11	0.062	C5–N11	1.440	1.025
	N13	13	0.001	N9–N13	1.227	1.937
	C16	16	0.237	N11–C16	1.425	1.079
	C17	17	−0.145	C16–C17	1.508	0.946
	O18	18	−0.364	C16–O18	1.224	1.789
	C19	19	−0.089	N13–C19	1.449	1.006

The order of increasing stability of bonds is: C16–C17 < C3–N9 < C5–N11 < N11–C16 < N13–C19 < N9–N13. This means that the first cleavage bond is C16–C17 followed by C3–N9, N13–C19 and N11–C16. The most stable bonds are azo group (N9–N13) and C16–O18

Table 5 The molecular orbital calculation parameters of neutral form of dye II

Dye II, neutral form	Atom	Atom ID	Partial charge	Bond	Bond length/Å	Bond Order
	O8	8	−0.223	C2–O8	1.369	1.059
	N9[a]	9	0.008	C3–N9	1.452	0.988
	N11[a]	11	0.061	C5–N11	1.440	1.025
	N13[b]	13	−0.002	N9–N13	1.227	1.939
	C16[a]	16	0.238	N11–C16	1.425	1.077
	C17[a]	17	−0.145	C16–C17	1.508	0.946
	O18[b]	18	−0.363	C16–O18	1.224	1.790
	C19[a]	19	−0.082	N13–C19	1.450	1.005
	H30[a]	30	0.066	C22–Br25	1.868	0.967

[a] The weak bonds/long bond length and low bond orders

[b] The strong bonds/high bond order and lower bond length

The order of increasing stability of bonds is: C16–C17 < C22–Br25 < C3–N9 < C5–N11 < N13–C19 < N11–C16 < N9–N13. This means that the first cleavage bond is C16–C17, C22–Br25 followed by C3–N9, C5–N11, N13–C19, and N11–C16. The most stable bonds are azo group/N9–N13 and the highly stable bond C16–O18

Table 6 The calculated molecular orbital parameters of neutral form of dye III

Dye III, neutral form	Atom	Atom ID	Partial charge	Bond	Bond length/Å	Bond order
	O8	8	−0.202	C2–O8	1.364	1.077
	N9	9	0.002	C3–N9	1.444	1.021
	N11	11	0.063	C5–N11	1.441	1.022
	N13	13	−0.035	N9–N13	1.233	1.887
	C16	16	0.237	N11–C16	1.424	1.081
	C17	17	−0.145	C16–C17	1.508	0.946
	O18	18	−0.367	C16–O18	1.224	1.786
	C19	19	−0.118	N13–C19	1.445	1.016
	C26	26	0.050	C22–O25	1.379	1.039
	H27	27	0.029	O25–C26	1.406	0.985

The order of increasing stability of bonds is: C16–C17 < N11–C16 < O25–C26 < C3–N9 < N13–C19 < C5–N11 < N9–N13. This means that the first cleavage bond is C16–C17 followed by N11–C16, O25–C26, C3–N9 and N13–C19. The most stable bonds are azo group/N9–N13 and its neighbor bond C5–N11. Also there is another stable bond C16–O18

gas-phase species can be handled much more easily by quantum chemistry than those surrounded by solvent [25].

Thermal analysis of dye I (Scheme 1), shows two weight loss steps, first one occurs at temperature range 100–260 °C and exactly at 162.5 °C (as given by DTG); this step occurs as a result of rupture of the bond C5–N11 as one of the unstable bonds as given from MOCs in Table 4 to loose $–NCOCH_3$. The second weight loss occurs at range of 260–480 °C and exactly at 377 °C as a result of bond rupture of C19–N13 as one of the unstable bond due to the loss of $–C_6H_4$. These thermal decompositions steps are essentially related to stepwise decomposition of the weakest bond in the following order C16–C17 < C3–N9 < C5–N11 < N11–C16 < N13–C19 < N9–N13 as given by MOCs of dye I in neutral form (Table 4).

TA decomposition of compound II (p-bromo-o-phenyazo-p-acetoamidophenol, $C_{14}H_{13}N_3O_2Br$) show two processes (Fig. 1b). The first process occurs at the temperature range 25–360 °C (TGA) with experimental weight loss of 25.07% (calculated weight loss = 24.32%) with peak temperature at 282.9 °C (DTA). The second process occurs at the temperature range of 310–500 °C (TGA) with experimental weight loss of 18.02% (calculated weight loss = 17.72%) at peak temperature at 483.02 °C (DTA). PM3 calculation (Table 3) shows that the C22–Br25 bond is the lowest bond order = 0.967 and longest bond length = 1.868 Å. Bromine may get ruptured after combining with H (i.e., HBr). The subsequent fragmentation includes the rupture of $COCH_2$ radical which reacts with OH to form CH_3COOH molecule. The Scheme 2 is initiated by HBr loss forming [M-HBr] ($C_{14}H_{12}N_3O_2^+$) as a result of decomposition of the weakest bond C22–Br25 followed by the cleavage of C3–N9 < C5–N11 < N13–C19 < N11–C16 bonds, respectively as given by MOCs of dye II in neutral form (Table 5).

Table 7 The molecular orbital calculation parameters of neutral form of dye IV

Dye IV, neutral form	Atom	Atom ID	Partial charge	Bond	Bond length/Å	Bond order
	O8	8	−0.201	C2–O8	1.362	1.084
	N9	9	0.042	C3–N9	1.440	1.028
	N11	11	0.035	C5–N11	1.445	1.013
	N13	13	−0.066	N9–N13	1.232	1.886
	C16	16	0.237	N11–C16	1.434	1.042
	C17	17	−0.144	C16–C17	1.509	0.945
	O18	18	−0.351	C16–O18	1.220	1.825
	C19	19	−0.011	N13–C19	1.450	1.010
	H30	30	0.064	C22–N25	1.497	0.902
	H31	31	0.061	N25–O37	1.215	1.494
	H32	32	0.075	N25–O38	1.215	1.495

The order of increasing stability of bonds is: C22–N25 < N11–C16 < C16–C17 < C3–N9 < N13–C19 < N9–N13. This means that the first cleavage bond is C22–N25 followed by N11–C16, C16–C17, C3–N9 and N13–C19. The most stable bonds are azo group/N9–N13 and its neighbor bond C5–N11. Also there are other stable bonds C16–O18, N25–O38 and N25–O37 of nitro group

Scheme 2 Thermal decomposition scheme of dye II

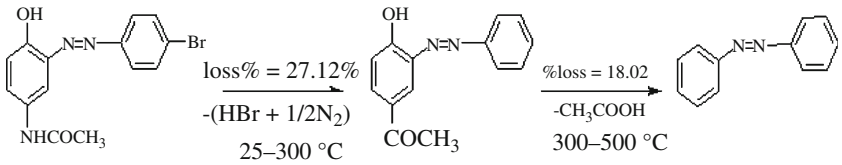

Scheme 3 Thermal decomposition scheme of dye III

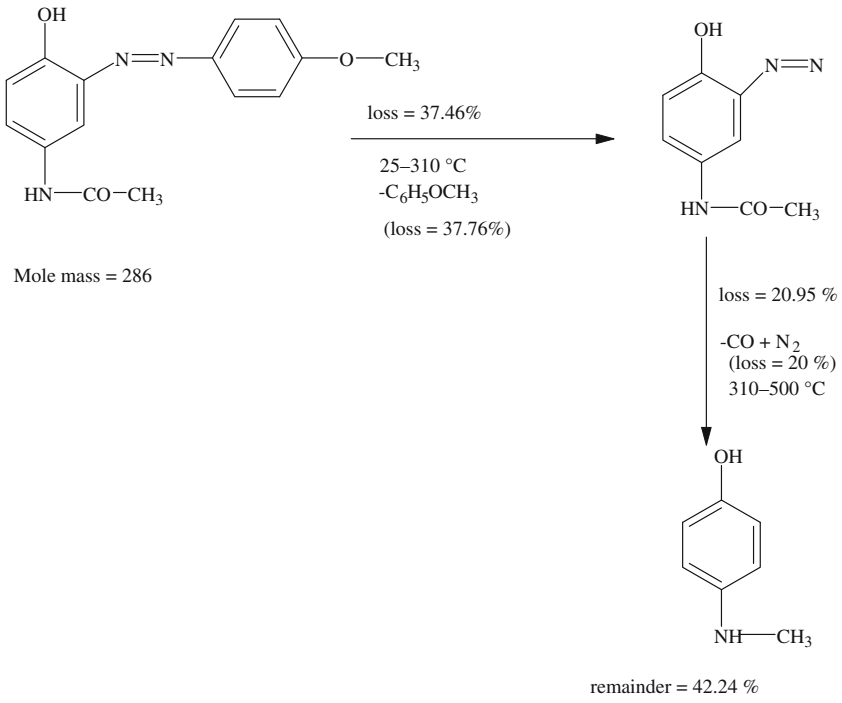

Thermal decomposition of dye III (Scheme 3) shows two steps; the first occurs at 25–310 °C due to the loss p-methoxyphenyl radical (Pract. Loss = 37.46% and Calcd. = 37.76%) and the second one occurs at 310–500 °C due to the loss of CO + N_2 gases (Pract loss = 20.95% and Calcd. = 20.0%). This essentially related to the decomposition of the weakest bonds coming from MOCs for the neutral form of the dye III (Table 6) C16–C17 < N11–C16 < O25–C26 < C3–N9 < N13–C19 < C5–N11 < N9–N13, respectively.

Scheme 4 Thermal decomposition scheme of dye IV

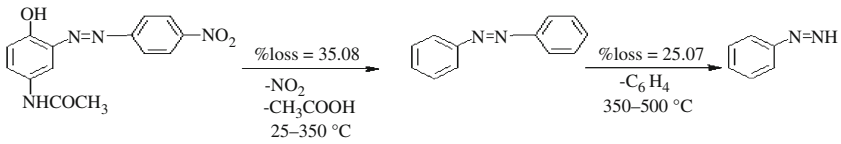

Thermal decomposition process of the dye IV (p-nitro-o-phenylazo-p-acetoamidophenol; $C_{14}H_{13}N_4O_4$) show two processes (Fig. 1a). The first process occurs at temperature range 25–360 °C with experimental weight loss of 35.08% (calculated weigh loss % at 35.0) with peak temperature at 287.03 °C (DTGA). The second process occurs at temperature range 360–500 °C with experimental weight loss of 25.07% (calculated mass loss % = 25.3) and peak temperature at 480.0 °C. Semi-empirical MO-calculation (PM3 procedure) shows from Table 2 that C22–N25 bond is the first site of bond rupture (lowest bond order = 0.902, longer bond length = 1.497 Å) leading to the NO_2 gas loss. Subsequent fragmentation includes rupture of $COCH_2$ radical. This radical reacts with OH to form CH_3COOH molecule. Therefore, the proposed thermal decomposition of the compound IV may be given by the following Scheme 4 as a result of decomposition of weakest bonds in the following order C22–N25 < N11–C16 < C16–C17 < C3–N9 < N13–C19 < N9–N13, respectively as given by MOCs results in Table 7.

Conclusions

The data obtained by mass and MOCs confirm each other and support the thermal decomposition schemes of these dyes by declaring the weak bonds and its sequence of bond rupture. It is generally concluded that thermal stability of these azodyes as a function of starting decomposition temperature and remaining of azo group till high-temperature range can be ordered as dye III < dye I < dye II < dye IV depending upon the Hammet's substituents values of −0.27, 0.01, 0.23, and 0.78, respectively (Table 3). The DTG values of the first fragmentation temperatures for dye III < dye I < dye II < dye IV are 274.16, 275, 282.9, and 287.83 °C, respectively. It is concluded that the primary fragmentation of compound III occurs exactly at 274.16 °C (from DTG) because of the loss of p-methoxyphenyl radical. Dye I also occurs exactly at 275 °C due to the loss of $NOCH_3$ group. Dye II starts at 25–300 °C (DTG, 282.9 °C) by the loss of HBr followed by CH_3COOH in two processes contrary to the behavior of compound I in which the two ruptures occur in one process. In case of dye IV, the first one appears exactly at 287.83 with practical mass loss % = 35.08. This loss may be attributed to the decomposition of NO_2 as a gaseous molecule together with an acetic acid molecule. These results agree well with Hammet's values and the given thermal stability ordering. The final weight losses of these dyes also occur in the same order of DTG values 475.55 °C (dye III), 377 °C (dye I), 448.3 °C (dye II), and 387.0 °C (dye IV), respectively. These values refer to the order of stability of the remainder parts keeping azo groups at elevated temperatures and decomposed in the second step. This also provides an important knowledge about the effect of temperature and thermal treatment of these dyes and consequently the temperature range of its thermal stability before going to decomposition. It also reveals the consequent fragments essentially obtained during fragmentation. These data can be used in industrial applications of these dyes in mordant dying processes.

References

1. Grayson M. Kirk-Othmer concise encyclopedia of chemical technology. Abridged version, 3rd ed. New York: Wiley; 1985.
2. Vlase T, Vlase G, Modra D, Doca N. Thermal behaviour of some industrial and food dyes. J Therm Anal Calorim. 2007;88(2):389–93.
3. Suprabha T, Haizel GR, Jesty T, Praveenkumar K, Suresh M. Microwave assisted synthesis of titania nanocubes, nanospheres and nanorods for photocatalytic dye degradation. Nanoscale Res Lett. 2009;4:144–52.
4. Wojciechowski K, Szadowski J. Thermal analysis of amide derivatives of *N*,*N*-dialkylaminoazobenzene. J Therm Anal Calorim. 1985;31(2):297–303.
5. Pinggui T, Yongjun F, Dianqing L. Improved thermal and photostability of an anthraquinone dye by intercalation in a zinc–aluminum layered double hydroxides host. Dyes Pigments. 2011;90(3):253–8.
6. Kocaokutgen H, Gümrükçüoğlu IE. Thermal characterization of some azo dyes containing interamolecular hydrogen bonds and non-bonds. J Therm Anal Calorim. 2003;71:675–9.
7. Larson BS, Meewen CN. Mass spectrometry of biological materials. New York: Marcel Dakker, Inc; 1998.
8. Euigyung J, Harold SF, Larry DC. Synthesis and characterization of selected 4,4′-diaminoalkoxyazobenzenes. Dyes Pigments. 2010;87(2):100–8.
9. Austin CA. To dissociate or decompose: investigating gas phase rearrangement of simple to complex compounds using mass spectrometry and thermal analysis. Ohio link Digital Resource (DRC); 2008.
10. Levsen K. Fundamental aspects of organic mass spectrometry. Weinheim: Verlag Chemie; 1978.
11. Bourcier S, Hoppilliard Y. Fragmentation mechanisms of protonated benzylamines. Electrospray ionisation-tandem mass spectrometry study and ab initio molecular orbital calculations. Eur J Mass Spectrom. 2003;9:351–60.
12. Fahmy MA, Zayed MA, Keshk YH. Comparative study on the fragmentation of some simple phenolic compounds using mass

spectrometry and thermal analyses. Thermochem Acta. 2001;366:183–8.
13. Fahmey MA, Zayed MA, El-shobaky HG. Study of some phenolic-iodine redox polymeric products by thermal analyses and mass spectrometry. J Therm Anal Calorim. 2005;82:137–42.
14. Mayer I, Gömöry Á. Semiempirical quantum chemical method for predicting mass spectrometric fragmentations. J Mol Struct. 1994;311:331–41.
15. Zayed MA, Fahmey MA, Hawash MF. Investigation of malomananilide and its dinitro-isomers using thermal analyses, mass spectrometry and semi-empirical MO calculations. Egypt J Chem. 2005;48(1):43–57.
16. Zayed MA, Fahmey MA, Hawash MF. Investigation of diazepam drug using thermal analyses, mass spectra and semi-empirical MO calculations. Spectrochim Acta A. 2005;61:799–805.
17. Zayed MA, Hawash MF, Fahmey MA. Structure investigation of codeine drug using mass spectra, thermal analyses and semi-empirical MO calculations. Spectrochim Acta A. 2005;64: 363–71.
18. Zayed MA, Fahmey MA, Hawash MF, El-Habeeb AA. Mass spectrometric investigation of buspirone drug in comparison with thermal analyses and molecular orbital calculations. Spectrochim Acta A. 2007;67:522–30.
19. Zayed MA, Nour El-Dien FA, Hawash MF, Fahmey MA. Mass spectra of gliclazide drug at various ion sources temperature. Its thermal behavior and molecular orbital calculations. J Therm Anal Calorim. 2010;102:305–12.
20. Hansch C, Leo A. Substituent constants for correlation analysis in chemistry and biology. NY: Wiley-Interscience; 1979.
21. Stewart JJP. Optimization of parameters for semiempirical methods. III Extension of PM3 to Be, Mg, Zn, Ga, Ge, As, Se, Cd, In, Sn, Sb, Te, Hg, Tl, Pb, and Bi. J Comput Chem. 1991;12:12320–341.
22. Baker J. An algorithm for the location of transition states. J Comput Chem. 2004;7(4):385–95.
23. Stewart JJP. MOPAC 2000. Tokyo, Japan: Fujitsu Limited; 1999.
24. Loew G, Chadwick M, Smith D. Applications of molecular orbital theory to the interpretation of mass spectra. Prediction of primary fragmentation sites in organic molecules. Org Mass Spectrom. 1973;7:1241–51.
25. Somogyi Á, Wysocki VH, Mayer I. The effect of protonation site on bond strengths in simple peptides: application of ab initio and modified neglect of differential overlap bond orders and modified neglect of differential overlap energy partitioning. J Am Soc Mass Spectrom. 1994;5:704–17.